PHYSICAL REVIEW A VOLUME 35, NUMBER 4 FEBRUARY 15, 1987

Magnetostatic trapping fields for neutral atoms

T. Bergeman
Physics Department, SUNY, Stony Brook, New York 11794

Gidon Erez
Physics Department, Ben Gurion University, Beer Sheva, Israel

Harold J. Metcalf
Physics Department, SUNY, Stony Brook, New York 11794

(Received 15 May 1986; revised manuscript received 14 November 1986)

In view of the recent successful confinement of decelerated sodium atoms in a magnetostatic trap, it is of interest to evaluate possible trap-field configurations. Neutral atoms in a Zeeman sublevel whose energy increases with field can be confined by a field whose magnitude $|\mathbf{B}|$ increases with distance from the center. Because this same basic requirement applies also to traps for neutrons and for plasmas (in the guiding-center approximation), trap configurations developed previously for these purposes are of interest for neutral atoms. However, the desired properties differ considerably because of very different objectives and different behavior of very cold atoms as compared with hot plasmas. We characterize basic trap configurations using both the exact expressions for the field, and a multipole polynomial expansion that facilitates studies of symmetry properties and classical or quantum orbits. Polynomial terms for the field components are derived and coefficients obtained by comparison with Taylor-series expansions and by global fit. Contours of $|\mathbf{B}|$ for various trap configurations are also presented. Under certain restrictive conditions, $|\mathbf{B}|$, and hence the effective potential, can be made isotropic to second order.

I. INTRODUCTION

The availability of cold atoms confined in a magnetostatic trap[1] offers a new experimental tool that is potentially useful for high-resolution spectroscopy, for studying decays of long-lived species, for studies of neutral-atom collective effects such as Bose-Einstein condensation, and for collision studies that might benefit from low relative velocities. Until recently, the primary difficulty in realizing a trap for neutral atoms has been the very shallow confining potential that can be attained with convenient magnetic fields. The typical trap depth is only about 1 K, from the relation $T=\bar{\mu}\Delta B/k$, where $\bar{\mu}$ is the atom's magnetic moment, ΔB is the field difference between the lowest threshold and the trap minimum, and k is Boltzmann's constant. Magnetic trapping therefore depends on substantial cooling of a thermal atomic sample, and is inextricably connected with laser cooling techniques that have been developed recently.[2–5] In actually making use of a magnetostatic trap for neutral atoms, spectral shifts associated with the inhomogeneous magnetic field present another major difficulty. It may be feasible to deal with this problem by further cooling within the trap so that atoms of interest occupy a small region near the field minimum. Achieving this goal so as to realize the inherent possibilities is a formidable technical challenge at present. As a step in this direction, this report surveys the basic trap configurations and also presents convenient methods for representing the field and hence the potential seen by the trapped atom.

Antecedents for the present study of magnetostatic trapping fields are to be found in discussions of neutron traps, developed primarily by Paul and collaborators[6–8] and discussed also by several other authors,[9–12] and from the extensive literature on magnetic confinement of plasmas.[13–16] For both of these techniques, as for neutral-atom traps,[17] the confining force originates from the interaction between a magnetic moment and a nonuniform static field. As compared with the much deeper ion traps, this interaction is inherently weaker and furthermore depends on the maintenance of a given orientation of the moment with the local field. For neutrons and for neutral atoms, this implies that the particle remains adiabatically in a given Zeeman sublevel. For plasma ions, the magnetic moment is generated by cyclotron motion about the local field in the "guiding center" approximation. In either case, when the precession frequency (Larmor or cyclotron) is not large compared with the frequency of orbital motion, the desired orientation is lost and the particle is likely to escape. Because of this similarity, magnetic trap configurations devised for neutrons or for plasmas are of interest for neutral atoms. However, there are considerable differences in the physical situation and in the probable uses. Neutron traps are intended for storage and for decay measurements; neutron spectroscopy or collective effects are not at issue. In plasma confinement, primarily directed toward achieving conditions for nuclear fusion, the goal is normally to achieve maximum temperature (and density) rather than minimum temperature as is typically the case for neutral atom traps. This extreme contrast presents some quite different design considerations. For example, instead of large external coils, one can place the trapping coils for neutral atoms entirely within the vacuum system. This means also that the entire trap po-

tential is relevant for confinement, and the container walls need not be a factor. With cold atoms, furthermore, very low collision rates, generally negligible many-body effects, and slow orbital motion may lead to acceptable leakage rates over regions of low field, despite violation of the adiabaticity condition. For example, the quadrupole trap configuration (known as cusped geometry in plasma work[13–16]) has been demonstrated[1] to yield confinement times of a second or more for neutral atoms, but was rejected in the early stages of plasma studies because of losses at the center where the field is zero. In view of these very different circumstances, it is worth re-evaluating magnetostatic trap configurations previously considered for neutrons and for plasmas.

The configurations discussed here are all static traps with one central minimum in $|\mathbf{B}|$ so as to obtain maximum localization of the atoms. These are the configurations of interest for experiments that involve cooling atoms within the trap so that they tend toward the minimum. This excludes toroidal geometries which are in fact the predominant form for both neutron and plasma traps. It may be that a toroidal configuration with a resonance region could be used for neutral atom spectroscopy, for example, by producing multiple "Ramsey fringes." However, this leads to serious questions, such as velocity collimation, that have not been addressed as yet. Oscillating field traps, as proposed recently for hydrogen,[18] are also not included in the present discussion. Also outside the present discussion are optical traps produced by the laser field itself[19,20] which present very interesting possibilities because of the continual flux of photons from the trapped atoms. It may be argued that magnetostatic traps, with all their inherent difficulties, do present certain advantages. First, there is a well-defined potential, so that quantized translation modes are not obscured by light field fluctuations. Second, there is no optical heating from spontaneous decay of excited atoms.

One useful way of classifying magnetostatic trap configurations is according to whether the minimum value of $|\mathbf{B}|$ is zero or not. Configurations with $|\mathbf{B}|_{\min}\neq 0$ avoid the problem of Majorana (spin-flip) transitions near the field zero, but are somewhat more complex. In Sec. III we discuss in some detail two configurations with $|\mathbf{B}|_{\min}=0$ and two with $|\mathbf{B}|_{\min}\neq 0$. The quadrupole (two-coil or cusped field[13–16]) configuration was proposed for neutral particle trapping by Paul,[21] and employed by Migdal *et al.*[1] to trap sodium atoms. This design, shown in Fig. 1(a), has a simple, open structure with $\mathbf{B}=\mathbf{0}$ at the center due to opposed currents in the two coils. In the spherical hexapole (three-coil) trap, [Fig. 1(b)], also proposed by Paul and co-workers,[6–8] the current in the equatorial coil is equal but opposite to that in the two coils at $+45°$ and $-45°$ latitude. $|\mathbf{B}|$ varies quadratically (but not isotropically) with distance away from the zero at the center, in contrast to the linear variation that results from the two-coil trap. We also discuss two $|\mathbf{B}|_{\min}\neq 0$ configurations that happen to correspond to plasma confinement schemes developed in the 1960's most notably by Ioffe and collaborators[22] and by Damm *et al.*[23] The Ioffe trap [Fig. 1(c)], consisting of two coils plus a quadruple focusing field for lateral confinement, has recently been proposed by Pritchard[24] for neutral atom trapping and cooling. The second $|\mathbf{B}|_{\min}\neq 0$ configuration, discussed in Sec. III D, has coils wound on a sphere following very nearly the seams of a baseball.

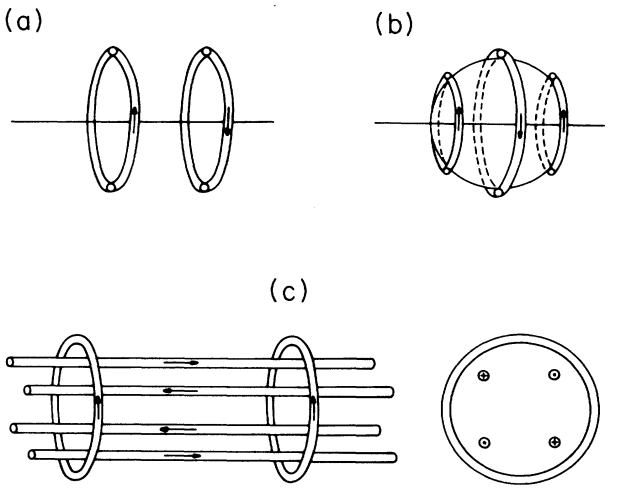

FIG. 1. Three magnetostatic trap configurations discussed in this work. (a) The magnetic quadrupole trap, consisting of two coils with opposing currents. (b) The "spherical hexapole" trap, with three wires on the surface of a sphere. With equal currents and the outer coils at 45°, $\mathbf{B}=\mathbf{0}$ at the origin. (c) The Ioffe trap, which has a bias field and axial confinement from a two-coil "bottle field" and transverse confinement from a four-wire quadrupole focusing field. Both side and end views are shown for the Ioffe trap.

If the atomic motion is adiabatic (without Majorana transitions to other Zeeman sublevels), it can be described by a local potential given by the atomic moment times $|\mathbf{B}|$. Particularly for motion near the center, a series expansion for $|\mathbf{B}|$ is useful for visualizing and calculating the orbits. In Sec. II, the respective orders of this expansion are identified with multipole terms. Coefficients are calculated with help of standard expressions for the field due to a current loop or straight wire. (The baseball trap requires numerical integration of the Biot-Savart law.) Very general considerations of these terms lead to insights about the limitations on magnetostatic fields imposed by Maxwell's equations. For example, these methods illustrate Wing's recent proof[25] that quasistatic magnetic (or electric) field magnitudes can have local minima but not local maxima. Because of this, static traps can only confine "weak field seeking" atoms. Furthermore, methods developed here show under what conditions an isotropic harmonic trap potential can be obtained (Appendix A and Secs. III C and III D). If the interest is in confinement properties over the entire trap volume, in addition to the multipole expansion parameters, contours of $|\mathbf{B}|$ are particularly useful and are therefore presented for each of the four configurations discussed below (Sec. III).

II. FORMULAS FOR THE TRAP-FIELD COMPONENTS

A. Exact expressions

The magnetic field from a coil is obtained by integrating the vector potential **A** over elements of each loop, and then applying $\nabla\times\mathbf{A}=\mathbf{B}$. For a single coil of radius R perpendicular to the z axis and centered at $z=A$, $B_\phi=0$, and the transverse and axial field components are[26,27]

$$B_z=\frac{\mu I}{2\pi}\frac{1}{[(R+\rho)^2+(z-A)^2]^{1/2}}\times\left[K(k^2)+\frac{R^2-\rho^2-(z-A)^2}{(R-\rho)^2+(z-A)^2}E(k^2)\right], \tag{1}$$

$$B_\rho=\frac{\mu I}{2\pi\rho}\frac{z-A}{[(R+\rho)^2+(z-A)^2]^{1/2}}\times\left[-K(k^2)+\frac{R^2+\rho^2+(z-A)^2}{(R-\rho)^2+(z-A)^2}E(k^2)\right], \tag{2}$$

where the argument of the complete elliptic integrals K and E is

$$k^2=\frac{4R\rho}{(R+\rho)^2+(z-A)^2}\ . \tag{3}$$

For a vacuum, in SI units (amps, meters, tesla), $\mu=\mu_0=4\pi\times10^{-7}$. (In "mixed" units amps, cm, gauss, $\mu_0=4\pi/10$.) The field from a long straight wire will be needed for the Ioffe trap configuration [Fig. 1(c)]. For a wire parallel to the z axis at cylindrical coordinates $\rho=S$, $\phi=\alpha$, one has $B_z=0$, and the other field components are

$$B_\rho=\frac{\mu I}{2\pi}\frac{S\sin(\phi-\alpha)}{[S^2+\rho^2-2S\rho\cos(\phi-\alpha)]}\ , \tag{4}$$

$$B_\phi=\frac{\mu I}{2\pi}\frac{S\cos(\phi-\alpha)-\rho}{[S^2+\rho^2-2S\rho\cos(\phi-\alpha)]}\ . \tag{5}$$

Equations (1)–(5) are needed to compute the trap depth and the field distribution far from the origin. However, approximate expressions in the form of low-order polynomial expansions are often useful in considering the symmetries of a given trap configuration. They are also useful in calculating classical trajectories, for which it is necessary to evaluate derivatives of the field at many points.

B. Multipole polynomial expansions

Maxwell's equations for a magnetostatic field in free space admit the existence of a scalar potential Ψ such that (in cylindrical coordinates)

$$\mathbf{B}=\nabla\Psi=\hat{\boldsymbol{\rho}}\frac{\partial\Psi}{\partial\rho}+\hat{\boldsymbol{\phi}}\frac{1}{\rho}\frac{\partial\Psi}{\partial\phi}+\hat{\mathbf{z}}\frac{\partial\Psi}{\partial z} \tag{6}$$

and

$$\nabla^2\Psi=0=\frac{\partial^2\Psi}{\partial\rho^2}+\frac{1}{\rho}\frac{\partial\Psi}{\partial\rho}+\frac{1}{\rho^2}\frac{\partial^2\Psi}{\partial\phi^2}+\frac{\partial^2\Psi}{\partial z^2}\ . \tag{7}$$

(For a single coil, Ψ is proportional to the solid angle subtended by the coil at the point of observation.) Solutions of (7) may be represented by a sum over spherical harmonics

$$\Psi=\sum_{L,M}a_{LM}r^LY_{LM}\ . \tag{8}$$

Each term in (8) corresponds to a magnetic multipole component analogous to those defined for radiative fields:[27]

$$\mathbf{B}_{LM}\cdot\mathbf{r}=r\frac{\partial\Psi_{LM}}{\partial r}=a_{LM}Lr^LY_{LM}\ . \tag{9}$$

The multipole expansion provides a useful means for classifying magnetostatic trap configurations. Note, however, that the multipole components of the field given in Eq. (9) are not simply related to fields arising from corresponding terms in the well-known multipole expansion of source currents. For example, $L=2$ components of B from (9), even when multiplied by r^{-5}, are not equivalent to the usual dipole field from an infinitesimal loop.

It is shown in Appendix B that for fields arising from just one L,M multipole component, those with $L>0$, $M=0$ are confining for an atom with a positive Zeeman coefficient, while for $M\neq0$ there is at least one line through the origin along which there is no confinement. The $M=L$, $L=1$, 2, and 3 fields are known as dipole, quadrupole, and hexapole deflection or focusing fields in atomic beam work.[28] The last two are useful in neutral atom traps for confinement in the transverse direction. However, fields from coaxial coils along the z axis, having no ϕ dependence, produce only $M=0$ multipole components and are of greatest interest here.

In view of the foregoing, we now restrict the discussion to $M=0$ and $|M|=L$ multipoles. Our immediate goal is to obtain convenient forms for the expansion of the field components. Because integrals over a sphere are not needed, the normalization of spherical harmonics is inconvenient. For the $M=0$ multipole terms, Legendre polynomials themselves are more suitable, particularly when written as polynomials in ρ and z:

$$\bar{\Psi}_{L0}=r^LP_{L0}(\cos\theta)=p_L(\rho,z)=\sum_{k=0}^{L}s_{Lk}\rho^kz^{L-k}\ . \tag{10}$$

The coefficients s_{Lk} may be obtained from standard expressions for Legendre polynomials. For high orders, it is simpler to apply (8) directly, noting that (a) first-order terms in ρ, and hence all odd k are excluded in order that $\nabla^2\Psi$ not diverge as $\rho\to0$, and (b) the coefficient s_{L0} of z^L in p_L is unity. For convenient reference, expressions for $p_L(\rho,z)$ are given in Table I. Also for the $|M|=L$ multipoles, we use (associated) Legendre polynomials:

$$\bar{\Psi}_{LL}=r^LP_{LL}(\cos\theta)e^{iL\phi}=(L-1)!!\rho^Le^{iL\phi}\ . \tag{11}$$

Field components are obtained by applying (6) to the above expressions. Because the order of each term decreases in going from Ψ to B, and to ensure the convenient expansion form

$$B_z(z,\rho=0)=\sum_{n=0}b_nz^n \tag{12}$$

we define new coefficients b_n, c_n, and d_n such that

TABLE I. Polynomial terms in the expansion of Ψ, $p_L = r^L P_{L0}(\cos\theta) = \sum_{k=0}^{L} s_{Lk} \rho^k z^{L-k}$; $s_{L0} = 1$.

L	p_L
0	1
1	z
2	$z^2 - \rho^2/2$
3	$z^3 - 3\rho^2 z/2$
4	$z^4 - 3\rho^2 z^2 + 3\rho^4/8$
5	$z^5 - 5z^3\rho^2 + 15z\rho^4/8$
6	$z^6 - 15z^4\rho^2/2 + 45z^2\rho^4/8 - 5\rho^6/16$
7	$z^7 - 21z^5\rho^2/2 + 105z^3\rho^4/8 - 35z\rho^6/16$
8	$z^8 - 14z^6\rho^2 + 105z^4\rho^4/4 - 35z^2\rho^6/4 + 35\rho^8/128$
9	$z^9 - 18z^7\rho^2 + 189z^5\rho^4/4 - 105z^3\rho^6/4 + 315z\rho^8/128$
10	$z^{10} - 45z^8\rho^2/2 + 315z^6\rho^4/4 - 525z^4\rho^6 + 1675z^2\rho^8/128 - 67\rho^{10}/256$

$$\Psi = \sum_{n=1} [b_{n-1} p_n(\rho,z) + c_{n-1}\rho^n \cos(n\phi) + d_{n-1}\rho^n \sin(n\phi)]/n \ , \tag{13}$$

and note that for configurations consisting only of coils centered on the z axis, all c_n's and d_n's are zero. Terms in b_n, c_n, or d_n correspond to $L = n+1$ multipoles. The field components now may be written

$$\begin{aligned} B_z &= \sum_{n=0} b_n B_{zn} \ , \\ B_\rho &= \sum_{n=0} b_n B_{\rho n} + \sum_{n=0} \rho^n \{c_n \cos[(n+1)\phi] + d_n \sin[(n+1)\phi]\} \ , \\ B_\phi &= \sum_{n=0} \rho^n \{-c_n \sin[(n+1)\phi] + d_n \cos[(n+1)\phi]\} \ . \end{aligned} \tag{14}$$

Expressions for B_{zn} and $B_{\rho n}$, computed from Eq. (4) and the polynomials in Table I, are given in Table II.

For a set of coaxial coils, b_n values may be obtained by considering the field along the z axis. Equation (14) (with $c_n = d_n = 0$) then give an expansion valid off the axis. Section II D below describes this procedure.

The radius of convergence of the series (12) for a coil of radius R centered at $z = A$ is $(R^2 + A^2)^{1/2}$ because there are poles of (1) (for $\rho = 0$) in the complex z plane at $z = A \pm iR$. It is also possible to consider a series expansion in ρ for $B_\rho(z=0,\rho)$. This series is quite tedious to compute by expanding Eq. (2), but from the expansions (14) one sees that the coefficients for $B_\rho(z=0,\rho)$ of the nth term will equal b_n times the coefficient of ρ^n in $B_{\rho n}$ (Table II). When the function $B_\rho(z=0,\rho)$ from Eq. (2) is considered in the complex ρ plane, it will be noted that each term, including the parameter k^2, has poles at $\rho = R \pm iA$ or $-R \pm iA$. Thus the radius of convergence of the series for $B_\rho(z=0,\rho)$ is also $(R^2 + A^2)^{1/2}$. Close to this limit, of course, the rate of convergence will be slow.

The absolute value of the field, $|\mathbf{B}|$, is of particular interest because it determines the potential for adiabatic motion (in which atoms remain in the same Zeeman sublevel). For the lowest nonzero order, one has

$$|\mathbf{B}|^2 = b_n^2 (B_{zn}^2 + B_{\rho n}^2) + (c_n^2 + d_n^2)\rho^{2n} + 2b_n B_{\rho n} \rho^n \{c_n \cos[(n+1)\phi] + d_n \sin[(n+1)\phi]\} \ . \tag{15}$$

If only coaxial coils are present, the lowest-order polynomials for $|\mathbf{B}|^2$ are

$$\begin{aligned} B_0 &= 1 \ , \\ B_1^2 &= z^2 + \rho^2/4 = r^2(\cos^2\theta + \sin^2\theta/4) \ , \\ B_2^2 &= z^4 + \rho^4/4 = r^4(\cos^4\theta + \sin^4\theta/4) \ , \\ B_3^2 &= z^6 - 3z^4\rho^2/4 + 3z^2\rho^4/2 + 9\rho^6/64 \ , \end{aligned} \tag{16}$$

etc., where $\theta = \tan^{-1}(\rho/z)$ is the azimuthal angle in spherical coordinates and $r = (z^2 + \rho^2)^{1/2}$ is the radial coordinate. For each n, we have $B_n = r^n f_n(\theta)$. Beyond lowest order, or when c_n or d_n are also nonzero, $|\mathbf{B}|$ is complicated by cross terms.

TABLE II. Polynomial terms in the expansion of B_z and B_ρ, $B_z = \sum_{n=0} b_n B_{zn}$ and $B_\rho = \sum_{n=0} b_n B_{\rho n}$.

n	B_{zn}	$B_{\rho n}$
0	1	0
1	z	$-\rho/2$
2	$z^2 - \rho^2/2$	$-\rho z$
3	$z^3 - 3z\rho^2/2$	$-3\rho z^2/2 + 3\rho^2/8$
4	$z^4 - 3z^2\rho^2 + 3\rho^4/8$	$-2\rho z^3 + 3\rho^3 z/2$
5	$z^5 - 5z^3\rho^2 + 15\rho^4 z/8$	$-5\rho z^4/2 + 15\rho^3 z^2/4 - 5\rho^5/16$
6	$z^6 - 15z^4\rho^2 + 45z^2\rho^4/56 - 5\rho^6/16$	$-33z^6 + 15\rho^3 z^3/2 - 15\rho^5 z/8$

C. General constraints on trap fields

The above form of the field expansions leads to certain useful conclusions. (a) Consistent with Wing's theorem,[25] the expansions (13) allow no maximum in $|\mathbf{B}|$ in an interior region. (b) There can be no nonzero minimum in $|\mathbf{B}|$ from current loops (b_n terms) alone. As illustrated by the Ioffe trap, if a uniform bias field is present ($b_0 \neq 0$), then a multipole term with $M \neq 0$ is needed to provide a potential barrier in all directions. (c) It is shown in Appendix A that for $|\mathbf{B}|_{\min}=0$ one cannot construct a magnetostatic trap with an isotropic harmonic variation of $|\mathbf{B}|$. Therefore, in any $|\mathbf{B}|_{\min}=0$ trap, the force vector $\bar{\mu}\nabla|\mathbf{B}|$ will not be radial except in certain preferred directions, and the atomic motion will not be harmonic in three dimensions. On the other hand, in a $|\mathbf{B}|_{\min}\neq 0$ trap, under special conditions defined in Sec. III D, the quadratic term can be isotropic. However, because of the constant term, the trap is then necessarily shallow and the higher-order terms make the region of isotropy very limited in extent. (d) In view of the foregoing, the total angular momentum of the atom in a trap is generally not conserved. However, in a trap consisting solely of coaxial coils, or in a pure $M=L$ multipole field (all $b_n=0$, one $c_n\neq 0$), the angular momentum along the z axis is conserved.

D. Methods for determining the expansion coefficients

The coefficients to be used in the multipole polynomial expansions may be determined either by matching coefficients with series expansions of Eqs. (1)–(5) near the origin, or by a fit to the global behavior of the field components over a volume of interest.

If the region near the origin is of interest, a Taylor series expansion is most natural. The simplest scheme to determine the coefficients is by reference to an expansion of the field component B_z along the z axis. For a circular coil of radius R, centered at $z=A$, carrying current I, the field along the axis is

$$B_z(z,\rho=0)=\frac{\mu IR^2}{2[R^2+(A-z)^2]^{3/2}}=\frac{\mu IR^2}{2(R^2+A^2)^{3/2}}\sum_{n=0} g_n(A,R)\left[\frac{z}{R^2+A^2}\right]^n. \tag{17}$$

The homogenous polynomials $g_n(A,R)$ are given in Table III for n up to 9 for later reference. For a set of coils, expansions of the form (17) are summed with appropriate values of I, R, and A for each coil.

In view of the radius of convergence discussed in Sec. II B, such a series converges very slowly near the transverse threshold for a set of coaxial coils. Therefore, if trap fields near the thresholds are needed, as for computing classical orbits in this region, optimum values of b_n are better determined by fitting exact expressions (1) to (5) over the region of interest. This procedure will be illustrated below for the two-coil trap.

III. CALCULATION OF B FOR SOME SIMPLE TRAP CONFIGURATIONS

As the simplest application of the expansion method, we consider a single coil at the origin. For $A=0$, we obtain from Eq. (17)

$$B_z(z,\rho=0)=\frac{\mu I}{2R}\left[1-\frac{3z^2}{2R^2}+\frac{15z^4}{8R^4}+\cdots\right]. \tag{18}$$

Values of b_n are determined by reference to Table II: $b_n=0$ for n odd, $b_0=\mu I/2R$, $b_2/b_0=-3/2R^2$, etc.

As a second introductory example, we consider two coils placed at $z=\pm A$, carrying the same current I, for which the field along the axis is

$$B_z(z,\rho=0)=\frac{\mu IR^2}{(R^2+A^2)^{3/2}}\times\left[1+\frac{3z^2(4A^2-R^2)}{2(A^2+R^2)^2}+\frac{15z^4(R^4-12A^2R^2+8A^4)}{8(A^2+R^2)^4}+\cdots\right]. \tag{19}$$

The Helmholtz configuration $A=R/2$ makes the quadratic term zero to achieve maximum field uniformity for two coils. It is straightforward by this method to arrange $2N$ coils to null out all terms z^{2n} (except z^0) for $n\leq N$. For $N>1$, $2N-1$ coils suffice if one coil is at $z=0$.

TABLE III. Polynomial terms in the expansion of $(R^2+A^2)^{3/2}/[R^2+(A-Z)^2]^{3/2}=\sum_{n=0} g_n z^n(R^2+A^2)^{-n}$.

n	g_n
0	1
1	$3A$
2	$3(4A^2-R^2)/2$
3	$5A(4A^2-3R^2)/2$
4	$15(R^4-12A^2R^2+8A^4)/8$
5	$21A(5R^4-20A^2R^2+8A^4)/8$
6	$-7(5R^6-120R^4A^2+240R^2A^4-64A^6)/16$
7	$-7A(35R^6-280R^4A^2+336R^2A^4-64A^6)/16$
8	$45(7R^8-280A^2R^6+1120A^4R^4-896A^6R^2+4132A^8)/128$
9	$5A(693R^8-9240R^6A^2+22176A^4R^4-126672R^2A^6+1408A^8)/128$

A. The two-coil (quadrupole) trap

Of more interest for trapping atoms is the two-coil configuration with opposed, equal currents. This configuration has a zero-field point at the center, a trapping potential that rises linearly from this point [the B_1 term in (16)], and saddle-point thresholds along the axis and in the plane midway between the coils. Here we will consider the ideal case of just two single loops. One possible criterion for the configuration of choice is that the threshold values of $|\mathbf{B}|$ along the z axis and in the $z=0$ plane be equal. This may not be optimum in practice because the atomic flux through these two regions will not be comparable. However, for our present purposes, this suffices to define a unique configuration. From Eqs. (1) and (2), we find that the threshold values of $|\mathbf{B}|$ are equal if the coils of radius R are centered at $z=\pm A$ with $A/R=0.626\,73$. The thresholds then occur at $\rho=0$, $z/R=\pm 0.7293$, and at $z=0$, $\rho/R=0.9530$. Contours computed for this configuration are shown in Fig. 2. In this and all subsequent figures, results are given for a specific current (100 A) and geometric size (coil radii of 1 cm), rather than in terms of dimensionless parameters, which are sometimes more cumbersome and less easily visualized. If all dimensions are scaled uniformly, fields will vary as I/R, derivatives as I/R^2, etc.

The low-order coefficients for the two-coil configuration are obtained by matching Eq. (14) with the sum of two series (19) with opposite signs of I and A. Values for the lowest-order parameters b_n, with numerical values for $A/R=0.626\,73$, are

$$b_1=\frac{3\mu IAR^2}{(R^2+A^2)^{5/2}}\rightarrow\frac{0.821\,27\mu I}{R^2}\,,$$
$$b_3=\frac{5(4A^2-3R^2)}{6(A^2+\rho^2)^2}b_1\rightarrow\frac{-0.504\,10\mu I}{R^4}\,. \tag{20}$$

Higher-order terms are easily obtained from Tables II and III. Near the origin, the equipotentials are ellipsoids of revolution about the minor axis. Because the ellipsoids are not confocal, the equations for classical or quantum motion do not separate in any of the standard ellipsoidal coordinate systems. As noted above for most magnetostatic trap configurations, the force $\bar{\mu}\nabla|\mathbf{B}|$ is not radial. However, for the lowest-order term the force in the radial direction is constant along any radial line because the potential is linear in r.

In computing classical orbits, the origin is a singular point because the force abruptly changes direction there. At this point the adiabatic assumption breaks down because atoms that pass very near the origin will experience a change in the orientation of the atomic moment relative to the local field direction (Majorana spin-flip transitions).

The limit of usefulness of polynomial expansions about the origin is indicated by the radii of convergence r_c of the series for $B_z(z,\rho=0)$ and $B_\rho(z=0,\rho)$. As mentioned above, in both cases $r_c=(R^2+A^2)^{1/2}$. For $A/R=0.626\,73$, $r_c/R=1.180$. The thresholds at $\rho=0$, $|z|/R=0.7293$ lie sufficiently within the circle of convergence that just five terms (up to z^9) reproduce exact values [from Eq. (1)] for $B_z(z,\rho=0)$ up through the threshold point quite well, as shown in Fig. 3(a). However, the threshold at $z=0$, $\rho/R=0.953$ is relatively closer to the radius of convergence, hence for $B_\rho(z=0,\rho)$, five terms are inadequate to reproduce the correct behavior at the threshold, as shown in Fig. 3(b).

By employing the polynomial expansion as a global approximation rather than a Taylor series expansion, it is

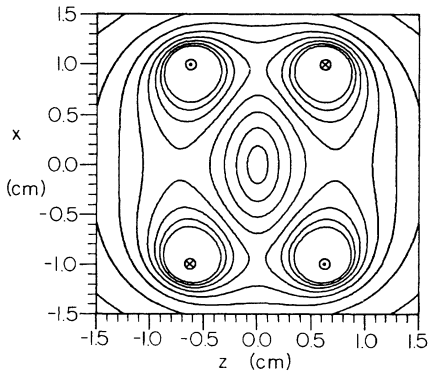

FIG. 2. Contours of $|\mathbf{B}|$ for the two coil "magnetic quadrupole" trap computed from Eqs. (1) and (2). Here $I=100$ A, $R=1$ cm, and $A=0.626\,73$ cm, chosen so that the thresholds along the z axis and between the coils ($z=0$) are of equal magnitude. The contours are drawn at 10 G intervals up to 80 G.

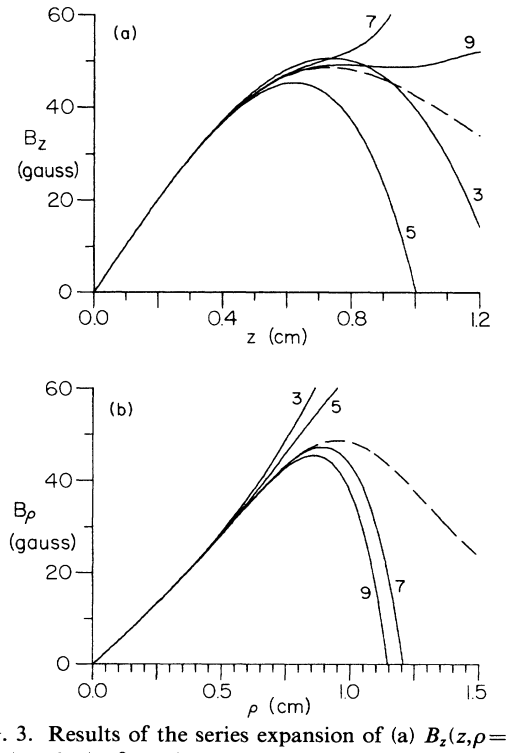

FIG. 3. Results of the series expansion of (a) $B_z(z,\rho=0)$ and (b) $B_\rho(z=0,\rho)$ for the two coil trap with $R=1$ cm, $A=0.626\,73$ cm. Coefficients are determined by comparison with the expansion of $B_z(z,\rho=0)$ about $z=0$. Solid curves are labeled by the maximum power of z or ρ, and dashed lines show the exact values calculated from Eqs. (1)—(3).

possible to reproduce the exact field values to good accuracy even beyond the threshold in ρ. For this purpose, we have used a least-squares procedure to fit b_n values to the exact functions $B_z(z,\rho=0)$ and $B_\rho(z=0,\rho)$. Figures 4(a) and 4(b) show that four terms (up to ρ^7 or z^7) serve to reproduce $B_z(z,\rho=0)$ and $B_\rho(\rho,z=0)$ quite accurately up to the thresholds in each case. To show how polynomial expansions behave off the axes, we show in Fig. 5 contours for the fitted four-term expansion (solid lines) superimposed on contours for the exact fields, as in Fig. 2 (shown as dashed lines in Fig. 5). In the well region, and even up the potential rise near the wires, the agreement is quite good. However, beyond the thresholds, the polynomial expansion has zeros which lead to sharp minima in $|\mathbf{B}|$ and produce the concentric circles on the contour plot. Classical orbit calculations performed with the analytic expansions therefore generally must terminate once the atom passes a threshold.

B. Three-coil (spherical hexapole) trap

With a three-coil configuration in which the field from the central coil opposes and cancels the field from the outer two coils at the origin, it is possible to produce a potential that varies as $r^2 f(\theta)$ near the origin. This may be advantageous in certain schemes for cooling the atoms within the trap.[29] The best known three-coil configuration is the "spherical hexapole" in which the three coils lie on a sphere and carry current of equal magnitude [Fig. 1(b)]. The name derives from the idea that in a plane containing the axis, three coils can be thought of as six wires (or six pole pieces) of a hexapole focusing magnet. Actually, according to the representation of Eq. (8) or (9), the field near the origin is a pole of order $L=3$, $M=0$, hence an octupole.

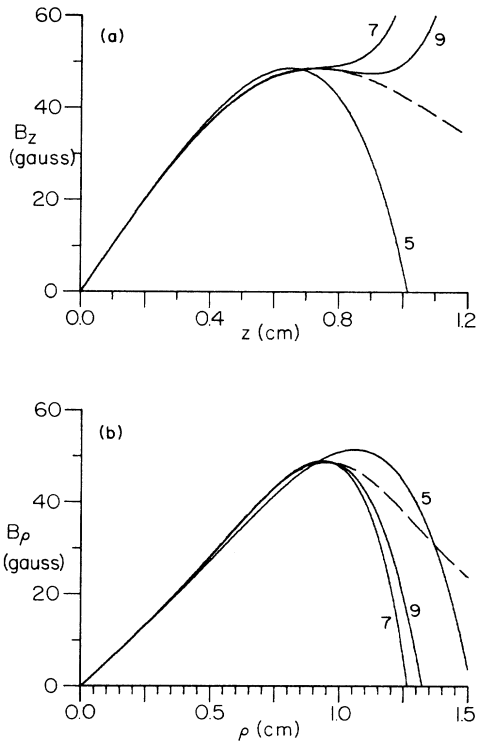

FIG. 4. Results from a polynomial expansion of (a) $B_z(z,\rho=0)$ and (b) $B_\rho(z=0,\rho)$ for the two-coil trap in which coefficients b_n have been determined by least-squares fit to the exact expression for $B_z(z,\rho=0)$ up to $z=0.75$ cm simultaneously with the expression for $B_\rho(z=0,\rho)$ for ρ up to 1.0 cm. As for Fig. 3, $R=1$ cm, $A=0.626\,73$ cm. Solid curves are labeled by the maximum power of z or ρ, and dashed lines give the exact values. These plots show that a polynomial expansion of relatively low order can be useful up to and beyond the threshold regions when the coefficients are determined by the global behavior of the fields.

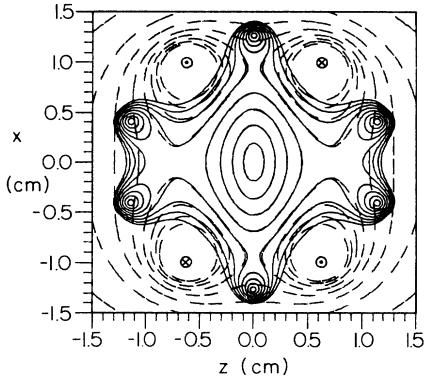

FIG. 5. Contours of $|\mathbf{B}|$ (solid lines) for the two-coil trap as a function of ρ and z calculated from the fitted four-term polynomial expansion as in Fig. 4 as compared with exact contours as in Fig. 1 (shown here in dashed lines). The concentric circles occur near zeros of $\mathbf{B}$, while the nearly circular dashed contours reflect rising $|\mathbf{B}|$ values near the wires. Contours are drawn every 10 G up to 80 G.

Field components near the origin can be computed by combining Eq. (19) for two coils with parallel current and Eq. (18) for a single coil centered at the origin. For a sphere of radius S, the two outer coils placed at $A=\pm S\cos\beta$ will have radius $R=S\sin\beta$, while the central coil at $A=0$ will have radius S. Thus along the axis, the field for equal currents I is

$$B_z(z,\rho=0)=\frac{\mu I(2\sin^2\beta-1)}{2S}+\frac{3\mu I z^2}{4S^3}[2\sin^2\beta(4\cos^2\beta-\sin^2\beta)+1]+\cdots \tag{21}$$

from which the b_n's are easily found by comparison with Eq. (12). The angle $\beta=\pi/4$ provides exact cancellation of the field at the origin so that the lowest term present is the b_2 term, and thus

$$|\mathbf{B}|=b_2 r^2(\cos^4\theta+\sin^4\theta/4)^{1/2}+\cdots, \tag{22}$$

where $b_2=15\mu I/8S^3$. Contours of $|\mathbf{B}|$ for the balanced spherical hexapole are shown in Fig. 6. Near the origin the shape is more angular than ellipsoidal, and the r^2 dependence makes the contour spacing unequal.

It is of interest to consider how the locus of points having $\mathbf{B}=\mathbf{0}$ behaves when the central coil does not precisely balance the outer two. For example, if $\beta=\pi/4+\delta$, we find that

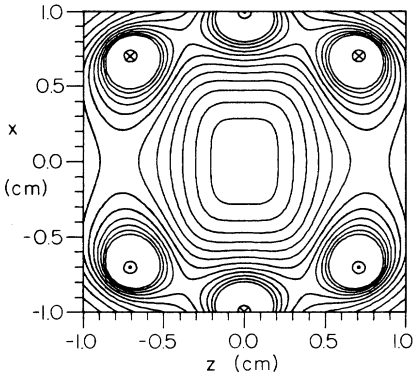

FIG. 6. Contours of $|\mathbf{B}|$ for the spherical hexapole trap on a sphere of radius 1 cm with currents of 100 A. Contours are shown in 10 G increments up to 120 G.

$$B_z(z,\rho=0)\cong\frac{\mu I\delta}{S}+\frac{3\mu I(5-4\delta)z^2}{8S^3}\ ,$$
$$B_z(z=0,\rho)\cong\frac{\mu I\delta}{S}-\frac{3\mu I(5-4\delta)\rho^2}{16S^3}\ . \tag{23}$$

[$B_\rho(z,\rho=0)$ and also $B_\rho(z=0,\rho)$ are zero.] The field geometry depends on the sign of δ. For $\delta<0$, $\mathbf{B}=\mathbf{0}$ at two points on the z axis and nowhere else. For $\delta>0$, $\mathbf{B}=\mathbf{0}$ on a ring in the $z=0$ plane. The potential surface near the origin is important when considering the motion of very cold atoms and in particular the quantized translation modes. The two-coil configuration always exhibits the same form near the origin if the coils are coaxial. If the current magnitudes or coil radii are not precisely equal, the origin shifts slightly from the midpoint. The form of potential surfaces for the three-coil configuration, however, depends sensitively on the balance between the coils.

Another three-coil configuration that may actually be more efficient places the three coils symmetrically on a cylinder. If the ratio of the current I_1 in the end coils at $z=\pm A$ to the current I_0 in the central coil is $I_1/I_0=-(1+A^2/R^2)^{3/2}$ the field will be zero at the origin.

C. The Ioffe trap

A trap consisting of two coils with parallel current and four straight conductors ("Ioffe bars") with current in alternating directions [Fig. 1(c)], has been used for plasma confinement[22] and has been proposed for neutral trapping by Pritchard.[24] Because of the nonzero minimum in $|\mathbf{B}|$, the Larmor frequency for even the coldest atoms can be made greater than the orbital frequency, so that the probability of spin-flip transitions is drastically reduced.

The field in this trap near the origin contains three multipole components: $M=0$, $L=1$ and 3, and $M=2$, $L=2$, with coefficients as defined above b_0, b_2, and c_1. Thus the field components near the origin are

$$B_z=b_0+b_2(z^2-\rho^2/2)+\cdots\ ,$$
$$B_\rho=-b_2z\rho+c_1\rho\cos(2\phi)+\cdots\ , \tag{24}$$
$$B_\phi=-c_1\rho\sin(2\phi)+\cdots\ ,$$

and therefore

$$|\mathbf{B}|^2=b_0^2+2z^2b_0b_2+b_2^2(z^4+\rho^4/4)$$
$$+\rho^2[c_1^2-b_0b_2-2c_1b_2z\cos(2\phi)]+\cdots\ . \tag{25}$$

In the $z=0$ plane, the field will be confining if $c_1^2>b_0b_2$. In view of the $\cos(2\phi)$ term, slightly higher values of c_1 are needed to confine for $z\neq0$. If higher multipole fields are used for lateral confinement, so that $c_1=0$ but, for example, the c_2 term is nonzero, then the coefficient of the ρ^2 in $|B|^2$ is $-b_0b_2$, which is necessarily opposite in sign to the z^2 term. Therefore for such fields there will be an annular region of minimum $|\mathbf{B}|$.

For the configuration of Fig. 1(c), the field from the coils alone near the origin is given by Eq. (19), from which b_0 and b_2 can be evaluated. Using Eqs. (4) and (5) for four infinite straight wires at $\rho=S$, $\phi_i=\pm\pi/4,\pm3\pi/4$ carrying current $I_1\tan\phi_i$, one finds $c_1=2\mu I_1/\pi S^2$. For a numerical example, easily scaled, we take $S=1$ cm and $R=1.5$ cm to allow for clearance, and place coils at $z=\pm A=\pm2.25$ cm. If trap dimensions are proportional to these figures, then when coil currents equal the currents in the straight conductors, the transverse field barrier in the plane midway between the straight wires is very nearly equal to the field barrier along z. Figures 7 and 8 show contours of $|\mathbf{B}|$ in the plane of two wires and midway between for 100-A current in the coils and in the straight wires. Under these conditions, the minimum field at the origin is 14.3 G, the axial threshold is 43.2 G, and the transverse threshold is about 44 G. There is a slight asymmetry for $\pm z$ in Fig. 8. For a plane perpendicular to the one chosen, the field contours will be reflected in the $z=0$ line. The long narrow central minimum approximates the "one-dimensional" harmonic well employed by Pritchard[24] in an optical-rf cooling scheme. It obviously can be made more one-dimensional by spreading the coils further apart. In a real trap, end effects of the straight wire components, effects of multiple turn coils, and finite wire size will modify the fields shown somewhat.

For certain purposes, it is desirable that the trap potential be harmonic and isotropic, so that the frequency of

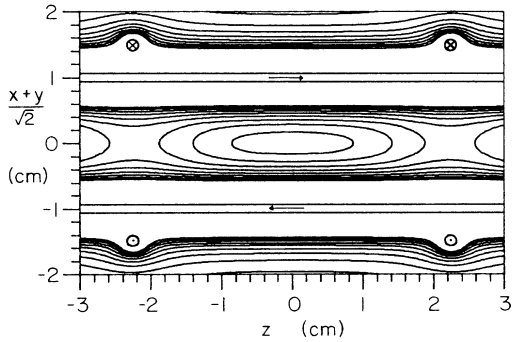

FIG. 7. Contours of $|\mathbf{B}|$ for the Ioffe trap of Fig. 1(c) in the plane of the straight wires. The four straight wires lie on a circle of radius 1 cm, the coils of radius 1.5 cm are spaced by 4.5 cm, and all currents are 100 A. The minimum field at the origin is 14.3 G. Contours are shown at 10 G intervals up to 100 G.

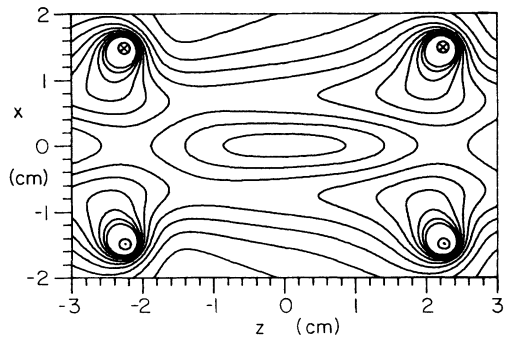

FIG. 8. Contours of $|\mathbf{B}|$ at 10 G intervals to 100 G in a plane midway between the straight wires for the Ioffe trap with parameters as given in Fig. 7. For a plane perpendicular to the one chosen, the contours will be as shown, but reflected in the $z=0$ line.

atomic motion is independent of direction. For example, this facilitates laser cooling procedures[29] and also simplifies the level structure of the quantized translational motion. It is shown in Appendix A that an isotropic potential with $|\mathbf{B}|=0$ at the center is not possible. However, it may be seen from (25) that with $b_0 \neq 0$, the expansion of $|\mathbf{B}|$ near the origin will have an isotropic second-order term if $c_1^2 = 3b_0 b_2$, so that the coefficient of z^2 equals that for ρ^2. Generally, this isotropy is attained at the cost of much reduced trap depth. Without changing the geometry used for Figs. 7 and 8, it is possible to achieve this by increasing the current in the coils from 100 to 455 A, in which case there is a small region near the center, of radius about 3 mm, in which the equipotentials are nearly spherical. However, because the field variation over this small region is only about 1 G, only atoms of very low kinetic energy will experience this isotropic potential. Furthermore, the minimum field is now 65.1 G and the transverse threshold is just 72 G. If the two coils are placed within the bars, then the coil current required for isotropy is much reduced, but the volume of effective isotropy is also smaller. It therefore appears that at least with the Ioffe trap geometry, an isotropic trap potential is feasible in the limit of low temperatures rather than as a means to facilitate cooling to attain this limit.

D. The baseball trap

A magnetic trap configuration in which coils follow the pattern of seams on a baseball has been used for plasma confinement since at least 1966.[23] An earlier design developed by Taylor and Sweetman in England was dubbed a "tennis ball" trap.[23(b)] The "baseball II" trap, depicted in a standard plasma physics text,[30] was approximately 2 m in diameter and required special strength steels. A variant of the baseball geometry that is said to be more efficient is the so-called "yin-yang" configuration,[31] with two coils folded along orthogonal axes. As for the baseball trap, the **B** field distribution resembles two fish tails butted together with a 90° twist in between.[16,32] The practical considerations in constructing a baseball trap for neutral atoms have yet to be confronted. The present discussion concerns strictly the ideal case of a single thin wire conductor on the surface of a sphere.

In the present discussion, a "baseball seam" is defined mathematically as composed of four contiguous planar arcs on a sphere, oriented as shown in Fig. 9. The z axis is an axis of two-fold symmetry (or, more precisely, a four-fold rotation-reflection axis). Such a form has just one degree of freedom, which may be taken to be α, where the arc centers lie on vectors at angles $+\alpha$, $-\alpha$, $+\alpha$ and $-\alpha$ with respect to the x, y, $-x$, and $-y$ axes, respectively. For Fig. 9, α is chosen to be 20°. It may be shown by simple geometric construction that each arc has a radius $R(1-\cos^2\alpha)/2^{1/2}$, where R is the radius of the spherical surface, and subtends an angle $\chi = \pi + 2\eta$, where $\sin\eta = \sin\alpha/(2-\cos^2\alpha)^{1/2}$. The points of closest approach to the z axis will occur at a lattitude of $\pi/2 - \beta = \alpha + \cos^{-1}[(\cos\alpha)/\sqrt{2}]$, which attains the maximum of $\pi/2$ at $\alpha = \cos^{-1}(\frac{2}{3})^{1/2} = 35.26°$, hence $\eta < 30°$. An actual baseball corresponds approximately to $\alpha = 16°$, while the seams on a tennis ball correspond more nearly to $\alpha = 6°$.

For this trap, the expansion method discussed in Sec. II D is not applicable because the arcs are not complete circles. However, it is not difficult to compute the field by numerical integration of the Biot-Savart equation around the loop. (The computation is simplified by rotating axes so that each planar arc in turn lies in the x-y plane, rotating back, and adding.) A representation of the field is shown in Ref. 32. Here we emphasize the contours of $|\mathbf{B}|$ rather than the **B** vector field itself. Contour lines for 40 G, for a baseball radius of 1 cm, current of 100 A, and $\alpha = 20°$, are shown at the center of Fig. 9.

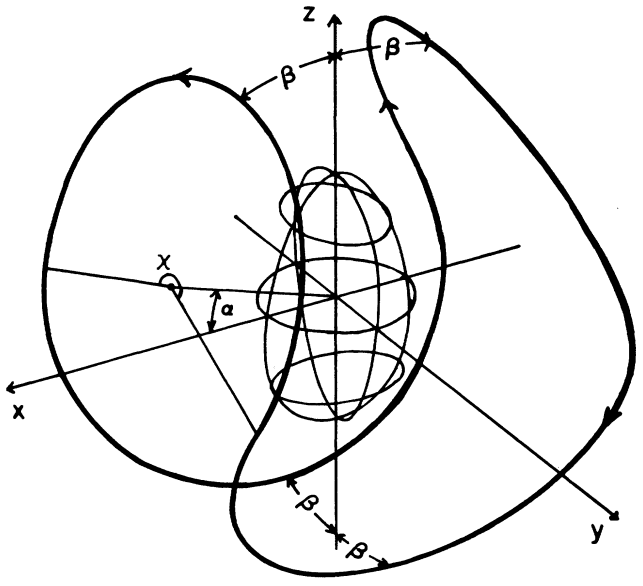

FIG. 9. The baseball coil (heavy line) with an equipotential surface shown schematically at the center. The coil consists of four contiguous planar circular segments, each subtending an angle χ, on axes at angle $\alpha(-\alpha)$ with respect to the $\pm x$ ($\pm y$) directions. At closest approach, the coil comes within angle β of the z axis. For this figure, $\alpha = 20°$ (hence $\beta = 21.6°$), and the contour lines represent a 40-G surface for a baseball of radius $R_B = 1$ cm, current $I_B = 100$ A.

They represent an asymmetric ellipsoidlike surface that has a circular cross section for $z=0$ and approximately elliptical cross sections for $z\neq 0$ with major axis along y for $z>0$ and along x for $z<0$. More extensive contours are shown in Fig. 10 for the same trap geometry and current. For $\alpha<\alpha_0=22.88°$, the **B** field along the z axis is everywhere in the same direction, but for $\alpha>\alpha_0$ the "jaws" of the coil lie sufficiently close to the z axis (e.g., in Fig. 9, β is sufficiently small) that the field is reversed at the poles relative to the center. There are therefore two points of null field along the z axis for $\alpha>\alpha_0$, and a single zero at the origin for $\alpha=\alpha_0$. Thus Fig. 11 shows that trap depth, defined as the value of $|\mathbf{B}|$ at the lower threshold (either along the z axis or in a perpendicular direction), less the value of $|\mathbf{B}|$ at the origin, increases up to $\alpha=\alpha_0$. Therefore in practice the optimum α value is as close to α_0 as is consistent with adiabatic motion at the origin. The $\alpha=0$ configuration, with four semicircular coils joined orthogonally, is easiest to construct but as seen from Fig. 11 is too shallow to be of interest.

The baseball trap can be construed as a Ioffe trap with the loops broken open and joined to the bars; the symmetry properties are similar. Just as for the Ioffe trap, the multipole expansion for the baseball trap at the origin is dominated by the $M=0$, $L=1$ and 3, $M=2$, $L=2$ terms. Multipole coefficients b_0, b_2, and c_1 are plotted versus α in Fig. 12. For $b_2>0$, $b_0<0$, the center is a saddle point rather than a minimum.

Because of the constraints on the multipole coefficients as indicated in Fig. 12, the balance condition for isotropy at the origin ($c_1^2=3b_0b_2$) can be obtained only by adding additional coils. By using two additional coaxial circular coils, for example, with a radius 1.25 times the baseball radius R_B, carrying the same current I_B as the baseball,

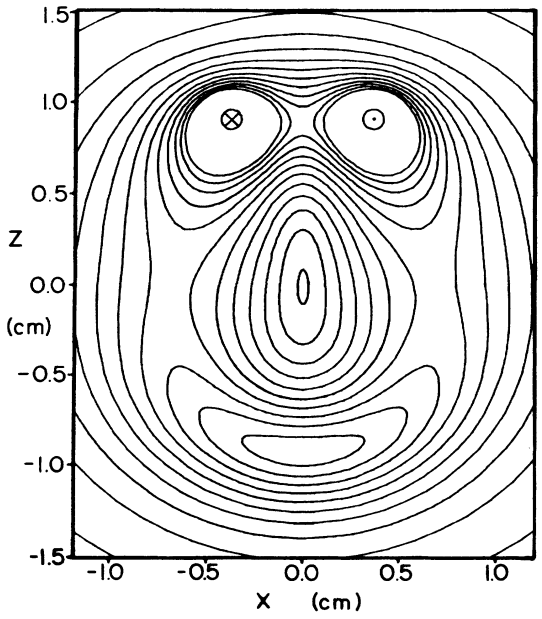

FIG. 10. Contours of $|\mathbf{B}|$ in the x-z plane of Fig. 9, with $\alpha=20°$ $R_B=1$ cm, and $I_B=100$ A. Contours are drawn at 10-G intervals. At the center, $|\mathbf{B}|_{\min}=9.1$ G, while the transverse and axial saddle-point thresholds are 72 and 106 G, respectively.

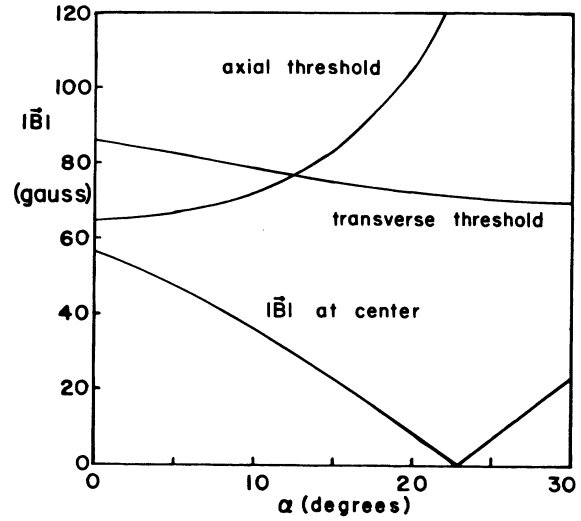

FIG. 11. $|\mathbf{B}|_{\min}$ and threshold field values for a baseball trap of radius $R_B=1$ cm and a current of 100 A as a function of the angle α (defined in Fig. 9). For $\alpha>23.88°$, the field at the center is directed oppositely to that at the poles.

the equipotentials can be made spherical to 5% out to a radius of $0.2R_B$ over a field variation of 6 G for the case of $I_B=100$ A, $R_B=1$ cm. Although the minimum is then raised to 61 G, the trap depth is 23 G under these circumstances. These figures are somewhat better than can be obtained with the Ioffe trap, but nevertheless, higher-order terms and the effect of the constant field

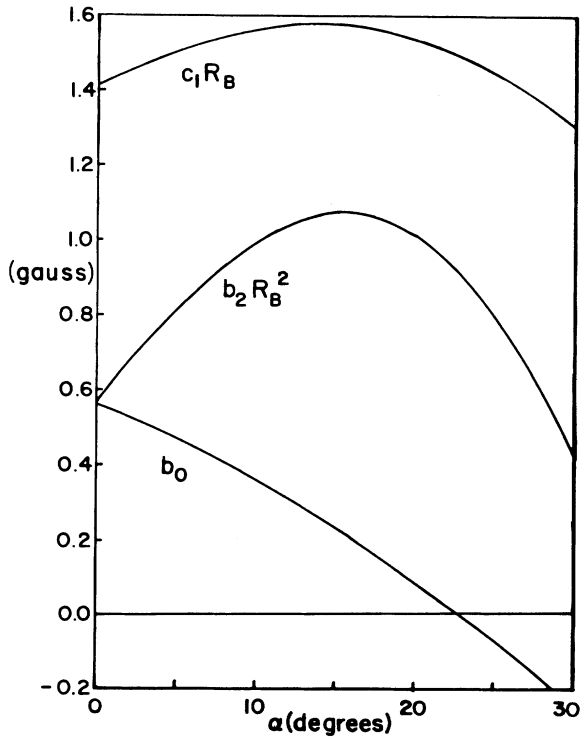

FIG. 12. Multipole expansion coefficients b_0, b_2, and c_1 for the baseball trap as a function of the angle α, for $R_B=1$ cm, and $I=100$ A.

considerably restrict the domain of isotropy.

The advantage of the baseball trap is the relatively open geometry (if the conductors need not be too bulky) and efficiency. On the other hand, the Ioffe trap has more flexibility because one can easily vary the spacing of the coils and the relative current in the bars and the coils.

IV. CONCLUSION

Magnetostatic traps for neutral atoms are potentially useful for previously unattainable precision spectroscopy and for the study of collective effects (possible "Bose-Einstein condensation") if means can be devised for further cooling of atoms in the trap. An understanding of classical and quantum atomic motion in an inhomogeneous magnetic field is clearly essential. As a first step, we have presented a method for analytic expansion of the trap field using polynomials derived from multipole terms, and we have applied this expansion method to several magnetostatic trap configurations that have been used for neutral atoms, neutrons, or plasmas. By knowing the relationship between multipole terms and the source currents, it is possible to design a trap to desired specifications, within the constraints of Maxwell's equations. An example is the design of a trap with an isotropic harmonic potential near the center, accomplished only with a substantial background field and at some sacrifice of trap depth. Computed contours of $|\mathbf{B}|$, such as we have presented for selected configurations, provide a useful representation of trap properties. Calculations of classical and quantum motion in trap fields are under way and will be presented in the future.[33]

ACKNOWLEDGMENTS

This work has been supported by the Office of Naval Research and by the National Science Foundation. We are indebted to Rolf Sinclair for making known to us previous investigations of magnetic traps for plasma confinement. T. B. acknowledges conversations with R. R. Lewis and Patrick McNicholl, particularly with regard to Appendix A, and with T. Kaiser and R. F. Post regarding traps for plasmas.

APPENDIX A

For the class of trap fields with $|\mathbf{B}|_{\min}=0$, we demonstrate that an isotropic, harmonic (r^2) trap potential is not possible.

In the multipole expansion of $|\mathbf{B}|$, the b_2 term from the P_{30} component, which produces a potential proportional to r^2, is clearly not isotropic [see Eq. (16)]. The question arises whether by some admixture of the other P_{3M} multipoles, an isotropic r^2 potential can be constructed. To examine this question, we take Ψ in the form

$$\Psi=r^3\sum_M a_M P_{3M}e^{iM\phi}\ , \tag{A1}$$

where the a_M are such that Ψ is real. In spherical coordinates

$$\mathbf{B}=\nabla\Psi=\hat{\mathbf{r}}\frac{\partial\Psi}{\partial r}+\hat{\boldsymbol{\theta}}\frac{1}{r}\frac{\partial\Psi}{\partial\theta}+\hat{\boldsymbol{\phi}}\frac{1}{r\sin\theta}\frac{\partial\Psi}{\partial\theta}\ . \tag{A2}$$

With help of the standard recursion relation, we have

$$\frac{\partial P_{LM}(\cos\theta)}{\partial\theta}=[(L+M)(L-M+1)P_{L,M-1}-P_{L,M+1}]/2\ , \tag{A3}$$

and therefore

$$\begin{aligned}|\mathbf{B}|^2r^{-4}=&9\left[\sum_M a_M P_{3M}e^{iM\phi}\right]^2\\&+\left[\sum_M a_M e^{iM\phi}[(3+M)(4-M)P_{3,M-1}\right.\\&\left.-P_{3,M+1}]\right]^2/4\\&-\left[\sum_M a_M Me^{iM\phi}P_{3M}\right]^2/\sin^2\theta\ .\end{aligned} \tag{A4}$$

Consider (A4) as a Fourier series in ϕ. For $|\mathbf{B}|$ to be isotropic, each independent term in $\exp(iN\phi)$, $0<N\leq 6$, must be zero. Considering terms with $N=\pm 6$, $N=\pm 4,\ldots$, successively, it is easily seen that the expressions multiplying $a_3^2,a_{-3}^2,a_2^2,a_{-2}^2,\ldots$ in each of these coefficient terms are not zero in general. For example, the coefficient of $\exp(6i\phi)$ is

$$a_3^2(P_{33}^2+9P_{32}^2-9P_{33}^2/\sin^2\theta)=-1800(\sin^6\theta)a_3^2\ . \tag{A5}$$

Hence one must have $a_3=0$, and similarly $a_{-3}=0, a_2=0,\ldots$ in order that there be no ϕ dependence. Finally, only the a_0 term is left, which is known to be anisotropic from (16).

On the other hand, if one does not demand that $|\mathbf{B}|_{\min}=0$, then as discussed in Secs. III C and III D, the $M=0$, $L=1$ and 3, and $M=2$, $L=2$ multipole components (b_0, b_2, and c_1 terms) can be combined in such a way as to give an isotropic variation of $|\mathbf{B}|$ to second order about the minimum.

APPENDIX B

We prove that magnetic fields from a single multipole component with $L>1$, $M=0$ are confining and that all other fields from a single L,M multipole are not confining.

For a single L,M multipole we have (for real Ψ)

$$\Psi=ar^LP_{LM}(\cos\theta)\cos(M\theta)\ , \tag{B1}$$

and from (8), the magnetic field is

$$\begin{aligned}\mathbf{B}/a=&\hat{\mathbf{r}}Lr^{L-1}P_{LM}(\cos\theta)\cos(M\theta)\\&-\hat{\boldsymbol{\theta}}r^{L-1}\sin\theta\frac{\partial P_{LM}(\cos\theta)}{\partial\cos\theta}\cos(M\theta)\\&-\hat{\boldsymbol{\theta}}r^{L-1}MP_{LM}(\cos\theta)\sin(M\phi)/\sin\theta\ .\end{aligned} \tag{B2}$$

Hence

$$|\mathbf{B}|^2 r^{2-2L} a^{-2} = L^2 P_{LM}^2 \cos^3(M\phi) + [(L+M)(L-M+1)P_{L,M-1} - P_{L,M+1}]^2 \frac{\cos^2(M\phi)}{4} + P_{LM}^2 M^2 \frac{\sin^2(M\phi)}{\sin^2\theta} . \quad \text{(B3)}$$

We first note that $L=1$ fields are uniform everywhere, hence nonconfining. If $L>1$, $M\neq 0$, then for $M\bar{\phi}=\pi(n+1)/2$ we have $\cos(M\bar{\phi})=0$, so that the first two terms in (B3) equal zero for $\phi=\bar{\phi}$. At θ such that $P_{LM}(\cos\bar{\theta})=0$, the third term is also zero. Hence along the radial direction defined by $\theta,\phi=\bar{\theta},\bar{\phi}$, the field is everywhere zero, hence nonconfining. On the other hand, for $L>1$, $M=0$, the third term in (B3) is zero and the first two terms are independent of ϕ. The first term is the sum of two squares, both of which cannot be zero. Hence there is no direction θ,ϕ for which $|\mathbf{B}|=0$. For $L>1$, $M=0$, $|\mathbf{B}|=0$ at the origin and nowhere else, and therefore the field is confining for atomic dipoles with a positive slope of energy versus field.

[1]A. Migdall, J. Prodan, W. Phillips, T. Bergeman, and H. Metcalf, Phys. Rev. Lett. **54**, 2596 (1985).

[2]W. Phillips and H. Metcalf, Phys. Rev. Lett. **48**, 596 (1982); J. Prodan, W. Phillips, and H. Metcalf, *ibid.* **49**, 1149 (1982); J. Prodan, A. Migdall, W. Phillips, I. So, H. Metcalf, and J. Dalibard, *ibid.* **54**, 992 (1985).

[3]W. Ertmer, R. Blatt, J. L. Hall, and M. Zhu, Phys. Rev. Lett. **54**, 996 (1985).

[4]S. Chu, L. Hollberg, J. Bjorkholm, A. Cable, and A. Ashkin, Phys. Rev. Lett. **55**, 48 (1985).

[5]W. Phillips, J. Prodan, and H. Metcalf, J. Opt. Soc. Am. B **2**, 1751 (1985). This is a review of laser cooling methods.

[6]K.-J. Kugler, K. Moritz, W. Paul, and U. Trinks, Nucl. Inst. Methods A **228**, 240 (1985).

[7]K.-J. Kugler, W. Paul, and U. Trinks, Phys. Lett. **72B**, 422 (1978).

[8]B. Martin, Dissertation, Universität Bonn-IR-75-8, 1975.

[9]V. Vladimirski, Zh. Eksp. Teor. Fiz. **39**, 1062 (1960) [Sov. Phys.—JETP **12**, 740 (1961)].

[10]C. V. Heer, Rev. Sci. Instrum. **34**, 532 (1963).

[11]I. M. Matora, Sov. J. Nucl. Phys. **16**, 349 (1973).

[12]R. Golub and J. Pendlebury, Rep. Prog. Phys. **42**, 445 (1979).

[13]N. A. Krall and A. W. Trivelpiece, *Principles of Plasma Physics* (McGraw-Hill, New York, 1973).

[14]*Magnetic Confinement*, edited by E. Teller (Academic, New York, 1981), Vol. 1, Part A.

[15]L. A. Artsimovich, *Controlled Thermonuclear Reactions* (Gordon and Breach, New York, 1964), translated from the Russian.

[16]R. F. Post, Nucl. Fusion (to be published). We are indebted to R. Sinclair for transmitting this reference to us.

[17]H. Metcalf, Prog. Quantum Electron. **8**, 169 (1984).

[18]R. V. E. Lovelace, C. Mehanian, T. J. Tommila, and D. M. Lee, Nature **318**, 30 (1985).

[19]A. Ashkin, Phys. Rev. Lett. **24**, 156 (1970).

[20]S. Chu, J. Bjorkholm, A. Ashkin, and A. Cable, Phys. Rev. Lett. **57**, 314 (1986).

[21]W. Paul (private communication). The use of this arrangement to trap neutral atoms was independently suggested by W. D. Phillips.

[22]Y. V. Gott, M. S. Ioffe, and V. G. Tel'kovskii, Nucl. Fusion, 1962 Suppl., Pt. 3, 1045 (1962).

[23](a) Physics Today **19**, 70 (1966); (b) J. Hiskes, Physics Today **20**, 9 (1967); (c) C. C. Damm *et al.*, in *Proceedings of the Third Conference on Plasma Physics and Controlled Nuclear Fusion Research* (Int'l Atomic Energy Agency, Vienna, 1969).

[24]D. E. Pritchard, Phys. Rev. Lett. **51**, 1336 (1983).

[25]W. Wing, Prog. Quantum Electron. **8**, 181 (1984).

[26]See, e.g., W. R. Smythe, *Static and Dynamic Electricity* (McGraw-Hill, New York, 1950).

[27]J. D. Jackson, *Classical Electrodynamics* (Wiley, New York, 1975). Equations (5.39) and (5.40) in this reference are incorrect because other terms of comparable order have been neglected. We are indebted to W. D. Phillips and E. R. Williams for pointing this out to us. (Reference 26 gives the correct forms.)

[28]N. Ramsey, *Molecular Beams* (Oxford University Press, New York, 1956); H. Friedburg, Z. Phys. **130**, 493 (1951).

[29]I. So, Thesis, Stony Brook, 1986 (unpublished).

[30]N. A. Krall and A. W. Trivelpiece, Ref. 13, p. 283.

[31]R. W. Moir and R. F. Post, Nucl. Fusion **9**, 253 (1969); F. L. Ribe, Rev. Mod. Phys. **47**, 7 (1975).

[32]R. A. Baldwin, Rev. Mod. Phys. **49**, 317 (1977).

[33]T. Bergeman, P. McNicholl, and H. Metcalf (unpublished).